OXFORD

Cerebral Cortex, 2023, **33**, 10367–10379
https://doi.org/10.1093/cercor/bhad288
Advance access publication date 16 August 2023
Original Article

Longitudinal developmental trajectories of functional connectivity reveal regional distribution of distinct age effects in infancy

Janelle Liu [1], Haitao Chen[1,2], Emil Cornea[3], John H. Gilmore[3], Wei Gao[1,4,*]

[1]Department of Biomedical Sciences, and Imaging, Cedars–Sinai Medical Center, Biomedical Imaging Research Institute, Los Angeles, CA 90048, United States,
[2]Department of Bioengineering, University of California Los Angeles, Los Angeles, CA 90095, United States,
[3]Department of Psychiatry, University of North Carolina Chapel Hill, Chapel Hill, NC 27514, United States,
[4]Department of Medicine, David Geffen School of Medicine, University of California, Los Angeles, CA 90095, United States

*Corresponding author: Biomedical Imaging Research Institute, Department of Biomedical Sciences and Imaging, Cedars–Sinai Medical Center, 116 N. Robertson Blvd., PACT 400.7G, Los Angeles, CA 90048, United States. Email: wei.gao@cshs.org

Prior work has shown that different functional brain networks exhibit different maturation rates, but little is known about whether and how different brain areas may differ in the exact shape of longitudinal functional connectivity growth trajectories during infancy. We used resting-state functional magnetic resonance imaging (fMRI) during natural sleep to characterize developmental trajectories of different regions using a longitudinal cohort of infants at 3 weeks (neonate), 1 year, and 2 years of age ($n = 90$; all with usable data at three time points). A novel whole brain heatmap analysis was performed with four mixed-effect models to determine the best fit of age-related changes for each functional connection: (i) growth effects: positive-linear-age, (ii) emergent effects: positive-log-age, (iii) pruning effects: negative-quadratic-age, and (iv) transient effects: positive-quadratic-age. Our results revealed that emergent (logarithmic) effects dominated developmental trajectory patterns, but significant pruning and transient effects were also observed, particularly in connections centered on inferior frontal and anterior cingulate areas that support social learning and conflict monitoring. Overall, unique global distribution patterns were observed for each growth model indicating that developmental trajectories for different connections are heterogeneous. All models showed significant effects concentrated in association areas, highlighting the dominance of higher-order social/cognitive development during the first 2 years of life.

Key words: brain; connectome; infant; rsfMRI; typical.

Introduction

Neurodevelopment during infancy is characterized by dramatic growth in the brain's functional architecture. Developmental trends consistently point toward increasing segregation (i.e. reduced short-range connectivity) as well as integration (i.e. increased long-range connectivity) as functional circuitry matures (Fair et al. 2009; Gao et al. 2009; Supekar et al. 2009; Uddin et al. 2010). However, the infant brain is remarkably plastic and modifiable during this developmental period (Gao et al. 2017; Ellis and Turk-Browne 2018), and there is substantial heterogeneity in how the functional connectomes of different brain regions develop (Gao et al. 2011). Indeed, prior work has robustly demonstrated a hierarchical timeline of maturation whereby different brain areas, networks, and processes mature at different rates across development (Kelly et al. 2009; Smyser et al. 2011; Gao et al. 2015b; Chen et al. 2021a). Whereas lower-order primary networks exhibit adult-like patterns at birth (Fransson et al. 2009; Smyser et al. 2010), higher-order networks undergo protracted development across the first few years of life, allowing for environment/experience to shape the development of these connections (Fransson et al. 2007, 2009, 2011; Fair et al. 2009; Gao et al. 2009, 2015b; Smyser et al. 2010, 2011; Grayson and Fair 2017). Although global patterns demonstrating varying maturational time courses are well established for canonical brain networks, little is known about the exact shapes of the growth curves and the detailed developmental trajectories of functional connectivity at the regional level during infancy.

Longitudinal functional magnetic resonance imaging (fMRI) research examining early neurodevelopment commonly treats age as a linear measure, but developmental change in neural function across many domains follows a variety of nonlinear patterns (Curran et al. 2010; Telzer et al. 2018; McCormick 2021; McCormick et al. 2021; Chen et al. 2021a). Indeed, prior studies examining functional development of distinct regions in the infant brain have demonstrated more dramatic changes during the first year of life than the second for different functional networks (Gao et al. 2009, 2015a, 2015b; Alcauter et al. 2015). This developmental trajectory is best captured by the log model rather than the more typical linear model. In previous studies, we directly compared linear and logarithmic models of growth for the development of insular (Alcauter et al. 2015), thalamocortical (Pendl et al. 2017), and canonical cortical network (Gao et al. 2015a) connectivity across the first 2 years of life. For these networks, the log model consistently demonstrated better fit as assessed by the Akaike Information Criterion (AIC). Subsequent work using the log model to examine the development of hippocampal (Liu et al. 2021) and amygdalar (Salzwedel et al. 2019a) connectivity revealed similar patterns of growth with

Received: December 5, 2022. **Revised:** July 13, 2023

dramatic increases in connectivity during the first year and limited changes in the second year of life. Overall, this indicates that higher-order regions may require postnatal environmental exposure to shape the development of their functional connections. However, some brain regions, including sensory (Pendl et al. 2017) and language (Emerson et al. 2016) areas, may establish functional connections with other regions with a mixture of linear, logarithmic, and quadratic trajectories. Despite this, most studies choose one polynomial (i.e. linear, quadratic) or logarithmic function for growth curve modeling, thus limiting the ability to better understand the heterogeneity of these developmental processes. Furthermore, most longitudinal fMRI studies examining early infant neurodevelopment have focused on specific regions of interest (Alcauter et al. 2015; Emerson et al. 2016; Pendl et al. 2017; Salzwedel et al. 2019a; Liu et al. 2021) or pre-defined cortical functional networks (Smyser et al. 2010; Gao et al. 2015a, 2015b). As such, little work has been at the whole-brain level to systematically assess the global distribution of different growth curve models across the entire brain. Taken together, this points to a significant gap in our understanding of the potentially different neurodevelopmental trajectories that optimally support functional growth of distinct brain regions during infancy.

In this study, we examined a cohort of 90 typically developing infants with three successful longitudinal resting-state fMRI (rsfMRI) scans at 3 weeks (neonate), 1 year, and 2 years of age. A functional parcellation-based heatmap analysis was used to delineate whole brain functional connectivity patters of neurodevelopmental trajectories optimally modeled by four growth curve models, including growth (positive-linear-age), emergent (positive-log-age), pruning (negative-quadratic-age), and transient effects (positive-quadratic-age). Next, ROI-level analysis was conducted to elucidate the underlying functional connectivity patterns best captured by each of the models. We expected to find unique patterns of age effects on the development of functional connectivity with a large proportion of emergent effects, given previous work demonstrating significant increases in the connectivity of many networks during the first year of life followed by tempered growth in the second year (Gao et al. 2009, 2015a, 2015b; Alcauter et al. 2015; Pendl et al. 2017; Salzwedel et al. 2019a; Liu et al. 2021). Given that this critical period is also a time of refinement based on environmental and experiential exposure (Smyser et al. 2011; Keunen et al. 2017), we hypothesized that pruning and transient effects would be observed in the development of connectivity for higher-order regions that undergo protracted development.

Materials and methods

Participants

Infant participants were part of the University of North Carolina Early Brain Development Study, characterizing early childhood brain and behavior development (Gao et al. 2017; Gilmore et al. 2018). We retrospectively identified 90 subjects with three successful rsfMRI scans during the first 2 years of life (at neonate, 1 year, and 2 years of age). Participant characteristics are listed in Table 1. Study protocols were approved by the University of North Carolina at Chapel Hill and Cedars-Sinai Institutional Review Board.

Table 1. Participant characteristics.

	$n = 90$
Sex (F/M)	47/43
Race (White/non-White)	56/34
Gestational Number (Singleton/Twin)	40/50
Atypical Development[a]	11
Mother Psychiatric Diagnosis	11
Mild Ventriculomegaly	2
Premature Birth (<37 weeks)	38
NICU Stay > 24 hours	26
Gestational Age at Birth (weeks)	36.37 (2.86)
Birthweight (grams)	2,665.56 (630.66)
Mother's Age at Birth (years)	29.96 (5.47)
Father's Age at Birth (years)	33.13 (7.00)[b]
Maternal Education (years)[c]	14.97 (3.66)
Neonate Scan	
Gestational Age at Scan (days)	293.51 (16.02)
Scanner (allegra/trio)	82/8
Mean rFD (mm)	0.09 (0.02)
One-year Scan	
Gestational Age at Scan (days)	654.06 (18.52)
Scanner (allegra/trio)	78/12
Mean rFD (mm)	0.09 (0.03)
Two-year Scan	
Gestational Age at Scan (days)	1,020.63 (20.80)
Scanner (allegra/trio)	64/26
Mean rFD (mm)	0.10 (0.03)

[a]Chiari malformation, later diagnosis with neurodevelopmental disorders such as autism spectrum disorder (ASD) or attention-deficit/hyperactivity disorder (ADHD). [b]N = 85. [c]At enrollment; NICU: neonatal intensive care unit; rFD: residual framewise displacement.

Imaging acquisition

Longitudinal rsfMRI data were acquired from the cohort of infants ($n = 90$) at 3 weeks (neonates), 1 year, and 2 years of age. Subjects were fed, swaddled, and fitted with ear protection prior to imaging. During the imaging session, all subjects were in a natural sleep state. All MRI data were collected on a Siemens 3 T Allegra (circular polarization head coil; neonates: $n = 82$, 1-year olds: $n = 78$, 2-year olds: $n = 64$) or Tim Trio scanner (32-channel head coil; neonates: $n = 8$, 1-year olds: $n = 12$, 2-year olds: $n = 26$). Scanner was included as a covariate of no interest in all subsequent analyses. Functional images were acquired using a T2∗-weighted echo planar imaging sequence: TR = 2,000 ms, TE = 32 ms, 33 slices, voxel size = 4 mm^2, 150 volumes. Structural images were acquired using a three-dimensional magnetization prepared rapid acquisition gradient-echo sequence: TR = 1,820 ms, TE = 4.38 ms, inversion time = 1,100 ms, voxel size = 1 mm^2. The acquisition parameters were identical for both scanners.

Data preprocessing

Functional imaging data were preprocessed using FMRIB's Software Library (Smith et al. 2004), Analysis of Functional Neuroimages (Cox 1996), and MATLAB (R2019a). Preprocessing included rigid-body motion correction, bandpass filtering (.01–.08 Hz), nuisance signal regression, and global signal regression. For the nuisance signal regression model, 32 parameters were included as nuisance regressors: eight regressors corresponding to mean white matter and mean cerebrospinal fluid time series in addition to 24 motion-related parameters (six motion correction parameters, their derivatives, their quadratic terms, and squared derivative terms; Power et al. 2014). All nuisance signals were bandpass filtered (.01–.08 Hz) before regression to match the frequency of the blood oxygen level-dependent signal. Data scrubbing was performed as an added motion correction step in addition to the standard rigid-body motion correction procedures. Volumes with framewise displacements higher than 0.3 mm were

removed ("scrubbed") from the data; one volume immediately preceding and two volumes following the scrubbed volume were also removed (Power et al. 2012). Subjects with fewer than 90 volumes remaining after scrubbing were excluded from the study. The residual framewise displacement (rFD) was compared cross-sectionally to ensure that there were no differences in motion; rFD was included as a covariate of no interest in all subsequent analyses. The data were spatially smoothed with a Gaussian kernel of 6 mm full width at half-maximum and truncated to 90 volumes. A supplemental analysis that included the entire length of data (i.e. all data available and not truncated to 90 volumes, with data length included as a covariate of no interest; Table S1) was conducted to ensure that truncation did not impact the results (see Supplementary Material). Briefly, whole brain heatmaps (methods described below) in the entire cohort using full length data were highly consistent with that using truncated data (Figs. S4–S7), indicating that truncation did not significantly influence the results. Thus, here we report findings using the truncated data. The University of North Carolina infant brain templates were used for co-registration (Shi et al. 2011). Specifically, spatial normalization to an infant brain template was achieved using a two-step approach (as recommended for pediatric datasets to improve accuracy and correct for changes in brain size; Cusack et al. 2018; Pfeifer et al. 2018): (i) subject-specific nonlinear functional-to-anatomical alignment followed by age-specific nonlinear anatomical-to-standard registration using Advanced Normalization Tools (ANTs; Avants et al. 2008), and (ii) between-age-group nonlinear transformation (using ANTs) to the 2-year template (Shi et al. 2011), which served as the final target for spatial normalization. Nonlinear warping using ANTs has been shown to be particularly effective for registering pediatric data (Sanchez et al. 2012) and each subject was visually checked to ensure good registration between time points.

Data analysis

Whole brain heatmap analysis

A whole brain heatmap analysis was designed to characterize developmental trajectories in functional connectivity. Functional connectivity measures were derived using a 2-year functional parcellation-based atlas (UNC-CEDARS INFANT; Shi et al. 2018). For each seed region of interest (ROI; $n = 278$), the average residual time series was extracted and correlated with every other ROI. In other words, a pairwise correlation between all ROIs was calculated across all 278 ROIs to form a 278×278 functional connectivity matrix for each subject. The correlation values were Fisher-Z transformed for subsequent statistical analyses. Next, for each ROI-to-ROI connection (i.e. seed ROI to all other 277 ROIs), four mixed-effect models were fit in MATLAB to determine the significance of four continuous age predictors (with Age defined as gestational age at scan), each assessing a distinct pattern of age-dependent change: (i) growth: positive-linear-age to model positive linear increases across neonate, 1 year, and 2 years of age and identify connections that experience consistent reinforcement across the first 2 years of life (Functional_Connectivity $\sim$ Age + Covariates, with the positive coefficient for Age as the main effect of interest; Fig. 1A); (ii) emergent: positive-log-age to model positive logarithmic increases across the first 2 years and identify connections that undergo dramatic change in the first year followed by tempered growth in the second year (Functional_Connectivity $\sim$ log(Age) + Covariates, with the positive coefficient for log(Age) as the main effect of interest; Fig. 1B); (iii) pruning: negative-quadratic-age to model inverted-U-shaped trajectories, which may be reflective of specialization processes that result from an initial over-proliferation of connections followed by refinement through experience-mediated pruning to retain only the necessary connections (Functional_Connectivity $\sim$ Age^2 + Age + Covariates, with the negative coefficient for Age^2 as the main effect of interest; Fig. 1C); (iv) transient: positive-quadratic-age to model U-shaped trajectories and identify regions that start with many connections but differentially respond to experience/refinement such that this initial pool of connections is followed by a substantial decrease during the first year and a subsequent recovery in connectivity by the end of the second year (Functional_Connectivity $\sim$ Age^2 + Age + Covariates, with the positive coefficient for Age^2 as the main effect of interest; Fig. 1D). It is important to note that since the infant brain develops dramatically across the first year of life and new connections grow accordingly (Smyser et al. 2011; Gao et al. 2015a), we focused on positive changes in functional connectivity for the growth and emergent models. In addition, it is important to highlight that the chosen names for each of the mixed-effect models presented here (growth, emergent, pruning, transient) are intended to describe system-level functional connectivity, which is not necessarily reflective of underlying cellular processes by the same name (particularly in the case of the pruning and transient model). In other words, we are not referring to cellular/molecular pruning and transient processes, but rather system-level functional connectivity changes that could be downstream of, but are distinct from, cellular/molecular pruning and transient processes.

The mixed-effect models included random intercept and slope terms with the effect estimate associated with age, log(age), positive quadratic age, or negative quadratic age being the principal variable of interest in each of the four mixed-effect models, respectively. Other participant characteristics were included as covariates of no interest, including scanner, sex, mean rFD, gestational age at birth, birthweight, twin status (i.e. whether or not the participant was part of a twin birth), atypical development (e.g. Chiari malformation, later diagnosis with neurodevelopmental disorders such as autism spectrum disorder [ASD] or attention-deficit/hyperactivity disorder [ADHD]), premature birth (defined as <37 weeks at birth), NICU stay (>24 hours), and maternal psychiatric diagnosis (e.g. with schizophrenia, bipolar disorder, major depressive disorder, or other psychosis). Of note, out of 50 participants who were part of a twin pair at birth, 24 were individuals who are twins but were the only twin of the pair included in the sample (due to data quality, etc.) and 26 were individuals who are twins and both twins were in the sample (i.e. 13 pairs of twins). Significance was defined as $P < 0.05$ and the AIC was used to determine which mixed-effect model was the best fit for the data. A summary measure defined as the percentage of significant connections (at $P < 0.05$) with the lowest AIC value normalized by the total number of possible connections (i.e. 277) was calculated and assigned to the seed ROI. This process was repeated for all ROIs to generate a heatmap such that the resulting heatmaps for each developmental model indicated the spatial distribution of age effects on functional connectivity. For completeness, a set of heatmaps displaying connections with significance defined as $P < 0.05$ but without using AIC as an additional criterion is presented in the Supplementary Material (Fig. S1). Finally, ROIs were grouped according to resting state network membership to qualitatively examine age-related changes at the network level using a seven-network parcellation (visual, sensorimotor, dorsal attention, ventral attention, limbic, frontoparietal, and default mode networks; Yeo et al. 2011) as well as a subcortical network (consisting of the remaining cortical regions including hippocampus, parahippocampal gyrus, amygdala, caudate, putamen,

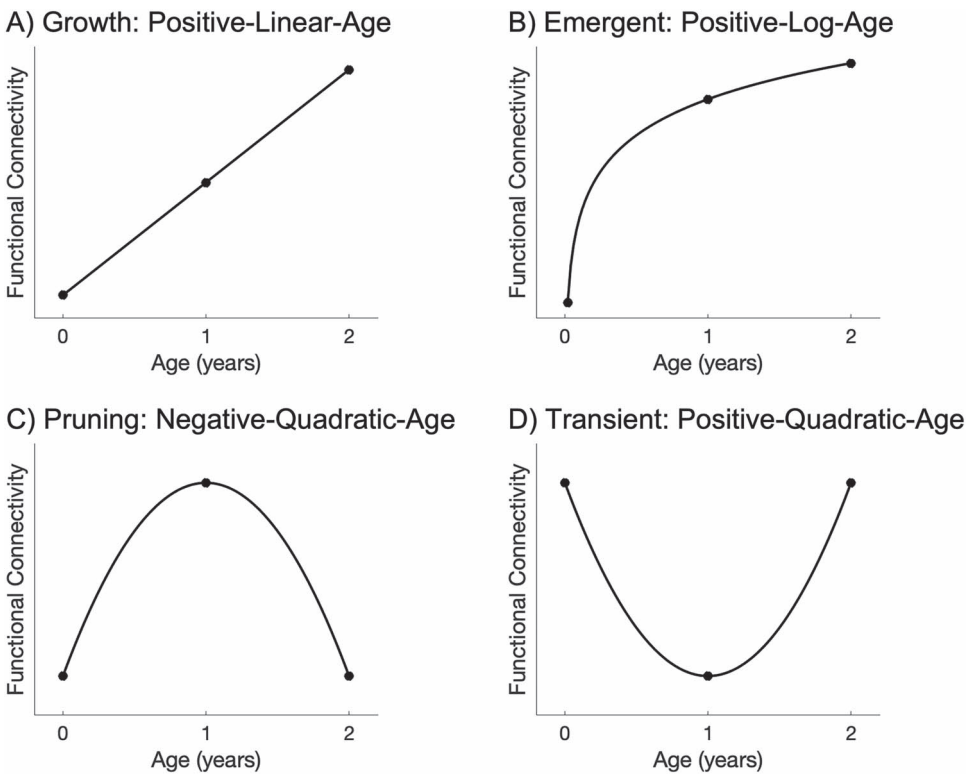

Fig. 1. Illustrative graphs charting the trajectory modeled by each age predictor in the four mixed-effect models examined. Growth effects, modeled by a positive-linear-age predictor, reflect connections that experience consistent reinforcement across the first 2 years of life (A). Emergent effects, modeled by a positive-log-age-predictor, reflect connections that undergo dramatic growth in the first year followed by tempered change in the second year of life (B). Pruning effects, modeled by a negative-quadratic-age predictor, reflect an initial over-proliferation of connections during the first year followed by experience-dependent refinement to retain only the necessary connections (C). Transient effects, modeled by a positive-quadratic-age predictor, reflect connections that start out strong but differentially respond to refinement such that these initial connections decrease during the first year and are followed by subsequent recovery in connectivity by the end of the second year (D).

pallidum, thalamus). It is important to note that the functional parcellation-based heatmaps were used (i) to provide a qualitative overview of the general distribution of the modeled age effects and (ii) as a data-driven screening to identify top-ranking ROIs showing the largest percentage of the modeled age effects, which were then selected for ROI-level analysis (described below). Lastly, given that preterm birth significantly impacts neurodevelopmental trajectories (Smyser et al. 2010; Lee et al. 2013; van den Heuvel et al. 2015; Pollatou et al. 2022), a supplemental whole brain heatmap analysis was conducted where infants were stratified based on term status ($n = 38$ preterm, $n = 52$ full term; Table S2; see Supplementary Material).

In addition to summarizing which models provided the best fit by summing connections across individual regions to generate the functional parcellation-based heatmaps, a connectivity matrix showing the best fit model for each individual connection was also generated (i.e. color-coding each individual connection by the best-fitting model). This was used to provide a qualitative overview of network-level phenomena.

ROI-level analysis

To elucidate the underlying functional connectivity patterns displaying each of the four mixed-effect models, the functional parcellation heatmaps for each model were used as a data-driven screening to identify the four highest-ranking ROIs showing the largest percentage of connections that were best fit by each model. ROI-level analysis was then conducted on the selected ROIs to identify significant patterns of connectivity showing these age effects within the network of the ROI. False discovery rate (FDR) correction (Benjamini and Hochberg 1995) with $p_{FDR} < 0.05$ was implemented across all connections with the lowest AIC value for that model to detect significant connections for each seed ROI. For better visualization, representative connections from each model are plotted showing data from all subjects with model fit curves overlaid (Fig. S15).

Results

Longitudinal age effects over the first 2 years of life

Heatmaps illustrating different age effects are shown in Fig. 2 and Fig. S2. It is important to note that these heatmaps were used as a data-driven screening to identify ROIs showing significant effects following FDR correction (described below) but are shown here to provide a qualitative overview of the general distribution of age effects. At the uncorrected level, growth effects (i.e. positive-linear-age) over the first 2 years of life were localized to higher-order frontal, parietal, and temporal regions, as well as anterior cingulate gyrus. These effects were least prevalent in visual and subcortical areas. Emergent effects (i.e. positive-log-age) were dominant in visual, temporal, parietal, and sensorimotor areas. These effects were least prevalent in temporal, subcortical, and mid-cingulate regions. Pruning effects (i.e. negative-quadratic-age) were localized to frontal and temporal areas as well as anterior cingulate gyrus. These effects were least present in primary temporal regions. Transient effects (i.e. positive-quadratic-age)

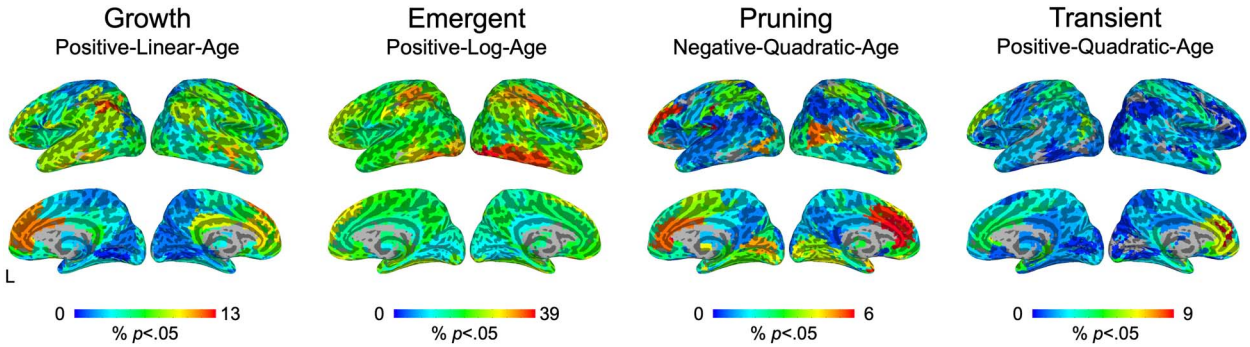

Fig. 2. Heatmaps of age effects. Qualitatively, heatmaps show unique patterns of age effects on brain connectivity across the first 2 years of life corresponding to growth (positive-linear-age), emergent (positive-log-age), pruning (negative-quadratic-age), and transient (positive-quadratic-age) effects. The color map and value of each ROI indicate the percentage of connections for this particular ROI (to every other functional parcellation ROI) showing significant connectivity based on *P*-value thresholding ($P < 0.05$) and the lowest AIC value across all four mixed-effect models. See Fig. S2 for an axial view and Fig. S3 for a standardized color range for quick comparison between models.

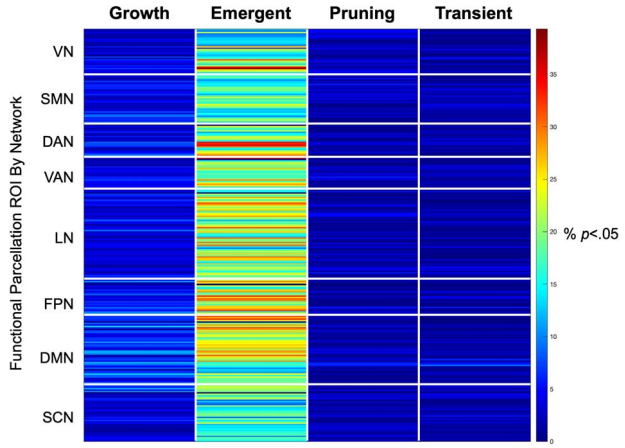

Fig. 3. Emergent age effects dominate. Across the four mixed-effect age models, the emergent (positive-log-age) model dominated growth trajectories in functional connectivity over the first 2 years of life. Along the y-axis, each row corresponds to one ROI (out of a total of 278 ROIs in the 2-year functional parcellation atlas), organized by resting state network membership. The color map and value of each cell indicates the percentage of connections for this particular ROI (to every other functional parcellation ROI) showing significant connectivity based on *P*-value thresholding ($P < 0.05$) and the lowest AIC value across all four mixed-effect models. VN: visual network; SMN: sensorimotor network; DAN: dorsal attention network; VAN: ventral attention network; LN: limbic network; FPN: frontoparietal network; DMN: default mode network; SCN: subcortical network.

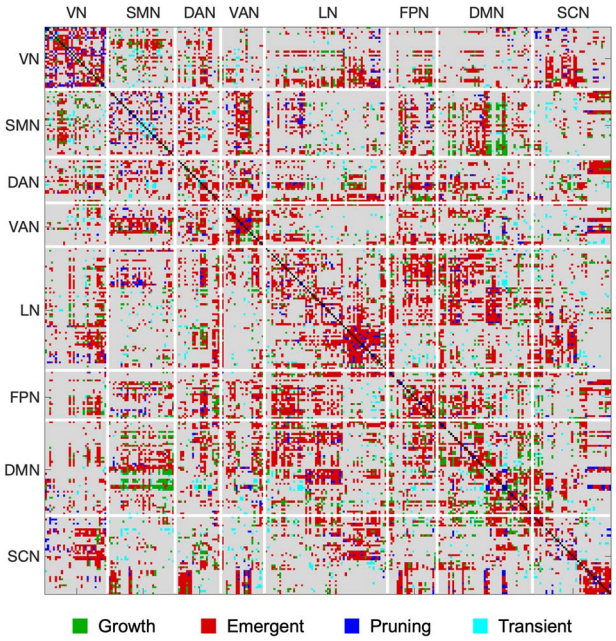

Fig. 4. Emergent age effects dominate within- and between-network connectivity. Across the four mixed-effect age models, the emergent (positive-log-age) model dominated growth trajectories in functional connectivity within and between canonical resting state networks. Emergent effects particularly dominated within-network connectivity for the VN, VAN, LN, DMN, and SCN as well as between-network connectivity between VAN-SMN, LN-FPN, and LN-DMN. In this connectivity matrix, each cell represents an individual connection between functional parcellation ROIs and is color coded to show the model that best fits that connection (significant connectivity based on *P*-value thresholding at $P < 0.05$ and the lowest AIC value across all four mixed-effect models). Connections for which there was no significant model fit are colored in gray; connections for which there was significant model fit are colored in green for growth (positive-linear-age), red for emergent (positive-log-age), blue for pruning (negative-quadratic-age), and cyan for transient (positive-quadratic-age) effects. VN: visual network; SMN: sensorimotor network; DAN: dorsal attention network; VAN: ventral attention network; LN: limbic network; FPN: frontoparietal network; DMN: default mode network; SCN: subcortical network.

were concentrated in orbitofrontal regions and anterior cingulate gyrus. These effects were lowest in temporal and subcortical areas. Across the four mixed-effect models, the emergent (positive-log-age) model best captured growth in connectivity (i.e. largest percentage of effects) over the first 2 years of life (Fig. 3). Indeed, at the qualitative level, the emergent (positive-log-age) model was dominant across both within-network connectivity (e.g. visual network, ventral attention network, limbic network, default mode network, subcortical network; Fig. 4) as well as between-network connectivity (e.g. ventral attention network–sensorimotor network, limbic network–frontoparietal network, limbic network–default mode network; Fig. 4).

ROI-level age effects

Growth (positive-linear-age) effects

Over the first 2 years of life, significant growth effects were concentrated in connectivity involved in socioemotional processing, integration, and salience detection (Table S3). The four highest-ranking ROIs showing the largest percentage of connections that were best fit by the linear growth model are shown in Fig. 5. This included linear increases in connectivity between: right superior frontal gyrus (dorsal; R SFGdor) and higher-order orbitofrontal

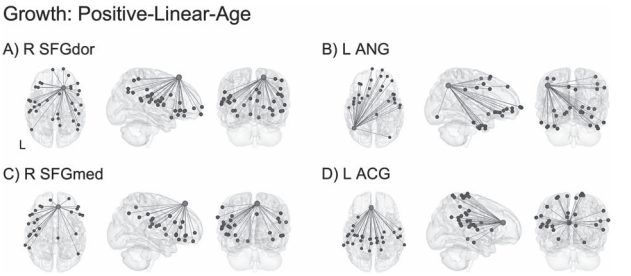

Fig. 5. ROI-level age effects: growth (positive-linear-age). Significant growth effects were localized to connectivity between regions involved in socioemotional processing (A), integration (B, C), and salience detection (D). Light gray spheres indicate seed ROI and dark gray spheres indicate significant connections surviving FDR correction. See Table S3 for a full breakdown of connections. For better visualization, a representative connection (R SFGdor–R ORBsup) is plotted showing single-subject scatterplots with model fit curve overlaid (Fig. S15A). R SFGdor: right superior frontal gyrus, dorsal; L ANG: left angular gyrus; R SFGmed: right superior frontal gyrus, medial; L ACG: left anterior cingulate gyrus; R ORBsup: right orbitofrontal cortex, superior.

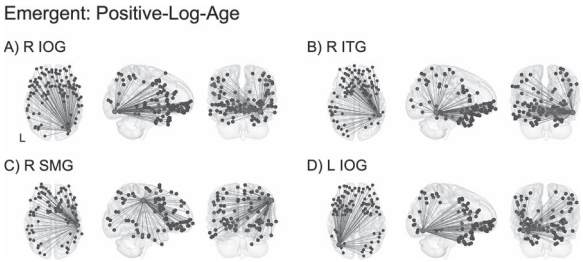

Fig. 6. ROI-level age effects: emergent (positive-log-age). Significant emergent effects demonstrated a consistent pattern of increasing long-range connectivity with higher-order frontal, limbic, subcortical, and parietal regions in addition to primary sensorimotor and visual areas. Connectivity between these regions is involved in sensory integration (A, B, D) as well as socioemotional processing (C). Light gray spheres indicate seed ROI and dark gray spheres indicate significant connections surviving FDR correction. See Table S4 for a full breakdown of connections. For better visualization, a representative connection (R IOG–L PreCG) is plotted showing single-subject scatterplots with model fit curve overlaid (Fig. S15B). R IOG: right inferior occipital gyrus; R ITG: right inferior temporal gyrus; R SMG: right supramarginal gyrus; L IOG: left inferior occipital gyrus; L PreCG: left precentral gyrus.

cortex (OFC) as well as subcortical regions (Fig. 5A); left angular gyrus (L ANG) and primary sensorimotor regions, middle cingulate gyrus, as well as higher-order frontal and temporal areas (Fig. 5B); right superior frontal gyrus (medial; R SFGmed) and higher-order frontal, parietal, temporal, and limbic regions (Fig. 5C); left anterior cingulate gyrus (L ACG) and primary sensorimotor, primary auditory, cingulate, and temporal areas (Fig. 5D).

Emergent (positive-log-age) effects

Significant emergent effects over the first 2 years of life revealed a consistent pattern of increasing long-range connectivity with higher-order regions involved in sensory integration and socioemotional processing (Table S4). The four highest-ranking ROIs showing the largest percentage of connections that were best fit by the logarithmic emergent model are shown in Fig. 6. Similar patterns of logarithmic increases in connectivity were observed between each of the four top-ranking ROIs and a constellation of distal regions including primary sensorimotor and visual areas as well as higher-order frontal, limbic, subcortical, temporal, and parietal areas. These patterns were remarkably similar for each of the four top-ranking ROIs including right inferior occipital gyrus (R IOG; Fig. 6A), right inferior temporal gyrus (R ITG; Fig. 6B), right supramarginal gyrus (R SMG; Fig. 6C), and left inferior occipital gyrus (L IOG; Fig. 6D).

Pruning (negative-quadratic-age) effects

Significant pruning effects following an inverted-U-shaped trajectory such that functional connectivity was highest at 1 year of age and "pruned" by 2 years of age were observed for connections between regions involved in salience detection, socioemotional processing, and integration (Table S5). The four highest-ranking ROIs showing the largest percentage of connections that were best fit by the quadratic pruning model are shown in Fig. 7. This included connectivity between: right anterior cingulate gyrus (R ACG) and higher-order frontal, cingulate, limbic, and subcortical areas (Fig. 7A and Fig. 6D); left Rolandic operculum (L ROL) and primary motor regions as well as higher-order frontal, parietal, and temporal areas (Fig. 7B); left inferior frontal gyrus, pars triangularis (L IFGtriang) and primary sensorimotor and visual regions in addition to higher-order frontal, limbic, and parietal areas (Fig. 7C).

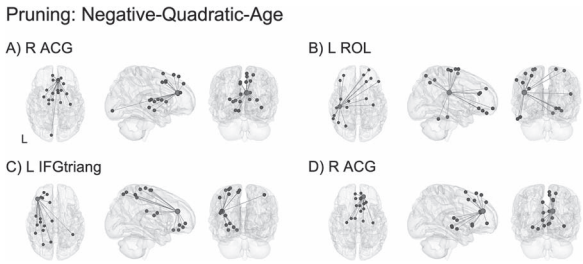

Fig. 7. ROI-level age effects: pruning (negative-quadratic-age). Significant pruning effects were observed in connectivity involved in salience detection (A, D; notably, two different functional parcellation locations within the right anterior cingulate gyrus), socioemotional processing (B), and integration (C). Light gray spheres indicate seed ROI and dark gray spheres indicate significant connections surviving FDR correction. See Table S5 for a full breakdown of connections. For better visualization, a representative connection (R ACG–R SFGdor) is plotted showing single-subject scatterplots with model fit curve overlaid (Fig. S15C). R ACG: right anterior cingulate gyrus; L ROL: left Rolandic operculum; L IFGtriang: left inferior frontal gyrus, pars triangularis; R SFGdor: right superior frontal gyrus, dorsal.

Transient (positive-quadratic-age) effects

Significant transient effects following a U-shaped trajectory such that functional connectivity was high at neonate, low at 1 year of age, and high again at 2 years of age were localized to similar ROIs as in the pruning model and concentrated in connections between regions involved in salience detection, higher-order processing, and integration (Table S6). The four highest-ranking ROIs showing the largest percentage of connections that were best fit by the quadratic transient model are shown in Fig. 8. This included connectivity between: R ACG and frontal, parietal, and temporal areas (Fig. 8A); right orbitofrontal cortex, medial (R ORBmed) and frontal, parietal, and temporal regions (Fig. 8B); R ACG and visual, frontal, and parietal regions (Fig. 8C); L IFGtriang and frontal, cingulate, and temporal areas (Fig. 8D).

Discussion

In this study, we characterized whole brain heatmaps showing the distribution of developmental changes in functional connectivity displaying growth (positive-linear-age), emergent

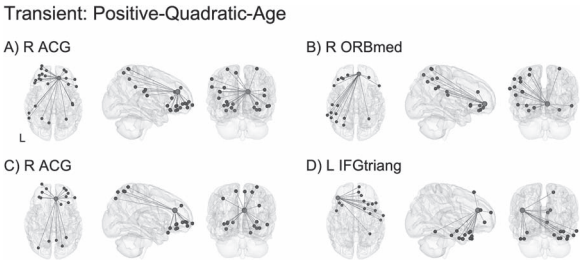

Fig. 8. ROI-level age effects: transient (positive-quadratic-age). Significant transient effects were localized to connectivity involved in salience detection (A, C; notably, two different functional parcellation locations within the right anterior cingulate gyrus) and integration (B, D). Light gray spheres indicate seed ROI and dark gray spheres indicate significant connections surviving FDR correction. See Table S6 for a full breakdown of connections. For better visualization, a representative connection (R ACG–L ORBmid) is plotted showing single-subject scatterplots with model fit curve overlaid (Fig. S15D). R ACG: right anterior cingulate gyrus; R ORBmed: right orbitofrontal cortex, medial; L IFGtriang: left inferior frontal gyrus, pars triangularis; L ORBmid: left orbitofrontal cortex, middle.

(positive-log-age), pruning (negative-quadratic-age), and transient (positive-quadratic-age) effects across the first 2 years of life. Distinct patterns of age effects on brain connectivity were observed, with the logarithmic emergent model demonstrating the largest percentage of effects across the developing brain. However, significant pruning and transient effects were also observed. ROI-level analysis revealed that age-related effects were localized to higher-order connections involved in socioemotional processing, integration, salience detection, and integration. Overall, our findings provide a better understanding of the heterogeneity within the hierarchical timeline of maturation for functional networks and indicate that different models of developmental change should be considered when examining longitudinal fMRI.

Global patterns of developmental trajectories

During infancy, primary functional networks (e.g. visual, auditory, sensorimotor) mature early on and are already synchronized at birth (Fransson et al. 2009; Smyser et al. 2010), whereas higher-order networks (e.g. salience, frontoparietal attention, default mode) undergo prolonged postnatal synchronization processes in the first few years of life (Fair et al. 2009; Gao et al. 2009, 2015a; Grayson and Fair 2017). This protracted developmental period allows for higher-order connections to be shaped by environmental exposure and experience-dependent refinement (Huttenlocher 1984; Toga et al. 2006; Keunen et al. 2017). However, different regions in the brain may require and/or experience different levels of exposure, which differentially affect neural plasticity of the functional connectome (Smyser et al. 2011; Keunen et al. 2017). Whereas some connections may be reinforced, leading to linear or logarithmic increases in connectivity, others may experience quadratic developmental trajectories (Telzer et al. 2018). In these models, connectivity profiles may undergo a specialization process and follow an inverted-U-shaped trajectory featuring rapid over-proliferation of connections followed by refinement through experience-mediated pruning to retain only the necessary connections (Gao et al. 2009). Still other connections may play a transient role during development in response to experience/environment and undergo a U-shaped trajectory starting with many connections followed by a substantial decrease and later increase in connectivity by the end of the second year. In line with prior work showing that different functional networks mature at different rates in the developing brain (Gao et al. 2015b), we observed unique patterns of age effects associated with each mixed-effect model. However, the emergent model (positive-log-age) was the dominant model among the four models examined with the largest percentage of effects across the entire brain. This is consistent with our prior work demonstrating that development of connectivity within various higher-order networks follows a logarithmic trajectory whereby more dramatic changes occur during the first than the second year of life (Gao et al. 2009, 2015a, 2015b; Alcauter et al. 2015; Pendl et al. 2017; Salzwedel et al. 2019a; Liu et al. 2021).

Since preterm birth is known to significantly impact neurodevelopmental trajectories (Smyser et al. 2010; Lee et al. 2013; van den Heuvel et al. 2015; Pollatou et al. 2022), a supplemental whole brain heatmap analysis was conducted where infants were stratified based on term status (see Supplementary Material). Overall age-related trends for each mixed-effect model were replicated within each subgroup (Figs. S8–S10) and the emergent model consistently dominated growth trends (Figs. S11). This is in line with our prior work using the novel BrainSync method (Joshi et al. 2018) to characterize voxelwise functional connectivity patterns from 0 to 6 years of age, where we detected similar global patterns of connectivity development in this same population of infants stratified by the term status (Chen et al. 2021a). It is important to note that the preterm infants we included were only moderately preterm with a mean gestational age of 33.61 weeks (range 30–36.86 weeks; Table S2), compared with very preterm infants examined in other studies (e.g. 26 weeks in Smyser et al. 2010; <32 weeks in Lee et al. 2013; 30 weeks in van den Heuvel et al. 2015). Thus, we may have been limited in detecting effects associated with preterm birth. However, the preterm subgroup qualitatively showed the largest effect sizes compared with the full-term subgroup as well as the entire cohort (Figs. S12–S14), suggesting that preterm infants may drive age-related effects observed in the entire cohort. Future work should be conducted in larger sample sizes to validate and extend these findings.

Distinct age effects

Growth effects (i.e. linear increases) were observed in functional networks of ROIs involved in higher-order cognitive processes, including socioemotional processing (R SFGdor), integration/attention (L ANG, R SFGmed), and salience detection (L ACG). These processes are important for identifying and processing salient information in the environment, which is critical for social learning and bonding during infancy (Atzil et al. 2018; Redcay and Warnell 2018). Consistent with prior work showing that functional circuitry underlying higher-order processes undergoes a protracted developmental period (Fair et al. 2009; Gao et al. 2009, 2015a; Grayson and Fair 2017), our findings indicate that synchronization of these higher-order connections increases linearly over the course of the first 2 years of life and may help support the early development of these processes.

Emergent effects (i.e. logarithmic increases) were localized to long-range connections in the networks of ROIs involved in sensory integration (R/L IOG, R ITG) and socioemotional processing (R SMG). More specifically, convergent connectivity patterns were detected between each of these ROIs and a consistent constellation of sensorimotor, visual, temporal, frontal, parietal, and limbic areas, indicating that integration across these regions dramatically increases across the first year with minimal changes during the second year of life. Notably, a large proportion of emergent effects were concentrated in connections between each of these ROIs and the OFC, a region that plays an important role in sensory

integration, socioemotional response, and reward processing to allow for adaptive responses to salient stimuli in the environment (Rolls et al. 2020). Work in animal models has robustly shown that neurons in the OFC are more sensitive to external factors such as visual cues (Bouret and Richmond 2010). In addition, the OFC is known to be heavily interconnected with sensory areas (Carmichael and Price 1995; Ongur and Price 2000), indicating that this region likely plays a role in integrating sensory information in response to processing salient stimuli from the environment to direct behavior. In line with this, three of the top-ranking ROIs showing the largest proportion of emergent effects were higher-order visual processing regions. This included bilateral IOG, which is involved in face processing (Sato et al. 2014; De Haas et al. 2021), and the right ITG, which plays a key role in the representation of objects and faces (Sato et al. 2013; Conway 2018). We also found a large concentration of logarithmic increases in connectivity between the right SMG, a region known to be involved in phonological processing and mediating emotional responses (Stoeckel et al. 2009; Hartwigsen et al. 2010; Silani et al. 2013), and OFC. Higher-order visual and phonological processing are crucial elements for supporting social learning during early development (Graven and Browne 2008). Our results support and extend the idea that the OFC is uniquely situated to integrate sensory information and modulate behavior in response to this input, demonstrating that dramatic synchronization of connections underlying these higher-order processes occurs in the first year of life with tempered growth in the second year. Furthermore, in line with prior work demonstrating that the maturational sequence of the functional connectome parallels the order in which behavioral and cognitive skills emerge and develop in early childhood (Keunen et al. 2017; Chen et al. 2021a), our findings provide a potential mechanism by which logarithmic increases in connectivity underlying higher-order visual/sensory integration may directly precede and support salience detection to facilitate learning.

Pruning and transient effects showed a joint picture of increases in both local differentiation as well as global integration in infancy, in line with previous work in typical development (Fair et al. 2009; Gao et al. 2009; Supekar et al. 2009; Uddin et al. 2010). At the synaptic level, this early critical period is characterized by remarkable plasticity which parallels the nonlinear developmental pattern of functional brain networks (Kelly et al. 2009). Early on, the over-proliferation of neurons is thought to serve as the basis for developing cognitive function by introducing early synaptic redundancy (Petanjek et al. 2008; DeMaster et al. 2019). However, synaptic pruning is equally important as it may enable more efficient communication between spatially distant brain regions to pave the way for the development of higher-order cognitive processes (Huttenlocher 1984, 1990; Toga et al. 2006). Interestingly, pruning and transient effects converged on the same three ROIs; one ROI in left inferior frontal gyrus pars triangularis (IFGtriang) and two ROIs in right anterior cingulate cortex (ACG) consistently emerged as the top-ranking ROIs showing the largest proportion of *both* pruning and transient effects across the first 2 years of life. For the left IFGtriang, local segregation was observed whereby intrahemispheric connections with ipsilateral sensorimotor, frontal, limbic, parietal, and visual regions were pruned. In addition, long-range integration featuring interhemispheric connections between left IFGtriang and mostly contralateral frontal, cingulate, and temporal areas were transient. Similarly, for the right ACG, short-range connections with nearby frontal, cingulate, limbic, and subcortical areas were pruned, whereas a mixture of short- and long-range connections between right ACG and nearby frontal regions as well as more distal parietal, temporal, and visual areas showed transient effects. Two distinct functional parcellation ROIs within the right ACG showed these patterns, highlighting the consistency of this developmental trajectory for this anatomical region. In addition to serving as a key node for salience detection (Menon and Uddin 2010; Uddin 2015), attention orientation (Schneider et al. 2020), and motivation/reward processing (Apps et al. 2016; Holroyd and Verguts 2021), the ACG is thought to play a particularly important role during development by facilitating learning through conflict monitoring (Palermo et al. 2018; Shapira-Lichter et al. 2018). Indeed, previous work has demonstrated that the ACG is essential for incorporating feedback from salient environmental and social information to assist with learning through trial and error (Burgos-Robles et al. 2019). During the first few years of life, these processes are crucial as infants are constantly learning—through trial and error—to differentiate information that is salient and worth attending. Accordingly, brain areas/connections supporting these activities may also need to undergo a trial and error process to establish optimal and effective connections, as featured in both the pruning and transient models observed in this study. Therefore, our results indicate that dynamic changes featuring both pruning and transient effects in the developing functional circuitry of the ACG may provide a potential mechanism for experience-dependent development for learning-related conflict monitoring processes in the infant brain.

Taken together, our ROI-level findings consistently revealed that age effects across the first 2 years of life differentially impact higher-order connections. Further, these age effects converged on connections involved in socioemotional processing, integration, and salience detection, which are interrelated processes that strongly influence one another to support social learning throughout development (Atzil et al. 2018; Redcay and Warnell 2018). This is in line with previous work showing that higher-order networks display dynamic changes and refinement during the first 2 years of life and are not fully mature until the end of adolescence (Solé-Padullés et al. 2016; Grayson and Fair 2017). Furthermore, networks associated with socioemotional processing in particular show the greatest developmental effects in adolescents (Kelly et al. 2009), indicating that these connections require a prolonged period of experience-dependent modulation that extends past infancy. During early development, the functional connectome of the infant brain changes continuously as a result of, and in interaction with, dramatic structural changes that are also occurring (van den Heuvel et al. 2015; Keunen et al. 2017). Thus, the functional changes we observed are likely the downstream effects of dynamic structural processes including cortical growth and synaptic remodeling that continuously reorganize and modulate neural circuits in this early critical period (Smyser et al. 2011). Taken together, our results indicate that functional connectivity underlying social learning is especially plastic and experiences a combination of different developmental trajectories, potentially in response to experience-dependent fine-tuning in the first 2 years of life. Our findings highlight the importance of examining different neurodevelopmental trajectories when charting longitudinal growth of the brain's functional connectome, particularly when these trajectories may be altered in different neurodevelopmental disorders or by exposure to environmental risk factors (Rogers et al. 2018; DeMaster et al. 2019).

Overall, our findings point toward a hierarchical timeline of maturation whereby different brain areas and processes mature at different rates across development. This has been observed

at the neuronal and synaptic levels, where different patterns of development are detected across different cognitive microcircuitries. Prior work in human postmortem brain tissue has shown that dendritic spine density is highest in childhood (Petanjek et al. 2011), which is a period of extensive dendritic growth with unique patterns of dendritic maturation distributed across different cognitive circuits (Petanjek et al. 2019). Paralleling the massive growth in functional connectivity observed here and in the developmental neuroimaging literature at large (see Pollatou et al. 2022 for a review), the majority of dendritic growth and synaptogenesis occurs during the first year (Ouyang et al. 2019) and may serve as the foundation for dramatic increases in functional connectivity (Hong and Park 2016; Bosch-Bayard et al. 2022). However, there has long been a debate on hierarchical versus synchronous maturation of cortical circuitry and a large body of work has examined synaptogenesis in the cerebral cortex to characterize the relationship between synaptic maturity and functional development (Rakic et al. 1994). There is some evidence for a hierarchical developmental pattern in the development of dendritic and spine systems of neurons in neonatal human neocortex (Travis et al. 2005), with more protracted development for supramodal regions compared with primary/unimodal regions. This is in line with the global patterns of development observed here as well as developmental trends across infancy and childhood characterized by early development of primary (lower-order) networks followed by protracted development of higher-order networks (Fair et al. 2009; Gao et al. 2009, 2015a; Grayson and Fair 2017). However, other evidence points toward a more synchronous model of maturation where there may be neuron classes that integrate information between several cortical areas and are part of a widely distributed network spanning across all cortical regions (Petanjek et al. 2008). Indeed, work examining synaptic development in rhesus monkey cerebral cortex has found more parallel maturation across cortical regions (Kovacs-Balint et al. 2021), but genetic analyses indicate that human-specific expression of synaptic genes in the prefrontal cortex is associated with synaptic functions (Liu et al. 2012), which may account for differences in cortical synaptic development between humans and other primates. In sum, our findings demonstrate that different areas in the brain undergo different maturational timelines, pointing toward a system-level reflection of underlying cellular and molecular processes that drive cortical maturation.

Limitations and future directions

Several limitations warrant further discussion. First, our goal in the present study was to compare between predetermined developmental trajectories (i.e. linear, log, quadratic). However, recent work has begun to explore more adaptable models of developmental change using spline modeling to investigate the best fitting function regardless of shape (Simmonds et al. 2017; Telzer et al. 2018). Although this approach affords a more flexible model of developmental change, spline models can be limited in terms of the interpretation linked to developmental theories and have the potential to overfit the data, thereby limiting the generalizability of the model beyond the sample at hand (Telzer et al. 2018). However, it is worth noting that spline modeling approaches would be able to account for linear/logarithmic decreases in connectivity as well, which were not explored in the present study. Future work should examine decreases in connectivity to more thoroughly characterize neurodevelopmental trajectories. Second, the rsfMRI data used in the present study were relatively short (3 min). Although rsfMRI data shorter than 10 min in length may have reduced reliability, prior work has shown that functional connectivity patterns are reliable and stable for scans between 3 and 12 min long (Van Dijk et al. 2010; Braun et al. 2012). We have previously used three minutes of rsfMRI data (i.e. 90 volumes in this dataset) to robustly detect brain connectivity in this same population of infants (Salzwedel et al. 2019b; Liu et al. 2021; Chen et al. 2021b, 2021a). Furthermore, our supplemental analysis demonstrated that full length rsfMRI data revealed a highly consistent distribution of age effects with that of truncated data (Fig. S6), indicating that data truncation did not significantly affect the present results. However, future large-scale studies with longer rsfMRI data will be able to fully address this limitation. Third, as the functional parcellation atlas was not created based on distinct growth patterns of various functional regions, our heatmap-based approach could have over-generalized growth patterns represented by each ROI and obscured diverse growth patterns exhibited by different connections stemming from the same ROI. However, the ROI-level analysis was aimed to elucidate underlying patterns to capture connectivity growth across various scenarios, including (i) one ROI with different subregions connected to different parts of the brain, and (ii) connections stemming from the same ROI following different patterns of growth. In other words, we used the ROI-level approach to characterize potentially diverse growth patterns exhibited by different connections stemming from the same ROI. Fourth, growing evidence has suggested that the timing of growth rates for various functional networks may be different between boys and girls during development (Scheinost et al. 2015; Gao et al. 2015b; Wheelock et al. 2019; Chen et al. 2021a). Future studies should take sex differences into consideration when examining developmental trajectories of functional connectivity. Fifth, environmental factors can have significant interactive effects that may alter developmental trajectories of the infant functional connectome (Graham et al. 2015; Gao et al. 2015a, 2019; Scheinost et al. 2017; Rudolph et al. 2018). More specifically, prenatal and perinatal exposures have significant impacts on early brain development and could have differential effects on brain growth trajectories (Dufford et al. 2021; De Asis-Cruz et al. 2022). In a supplemental analysis stratifying the entire cohort based on term status (full term and preterm), overall age-related trends were replicated within each subgroup and the emergent model was consistently best captured growth in connectivity. However, there were qualitative differences in the distribution of age-related effects based on term status. Future work should seek to investigate the moderating impact of various pre/postnatal factors that can confer risk as well as resilience throughout the course of development. Lastly, future work should endeavor to link the functional connections described here with behavioral outcomes to identify behavioral implications of early functional connectivity growth. It will be important to validate and extend these findings in population-level datasets with larger sample sizes (e.g. the HEALthy Brain and Child Development Study) with the ultimate goal of identifying altered neurodevelopmental trajectories and inform targeted interventions to optimize outcomes (Pollatou et al. 2022).

Conclusions

Consistent with previous findings showing dynamic functional connectivity development during infancy, we found unique patterns of functional connectivity growth distributed across the brain. Emergent (i.e. logarithmic) effects dominated developmental trajectory patterns during the first 2 years of life. Significant pruning and transient effects were also observed, particularly in social learning-related inferior frontal and anterior cingulate

areas, indicating that the functional connectivity underlying these higher-order cognitive/social processes experiences dynamic and variable changes in early development. These results suggest that different areas in the brain follow different maturational timelines at the system level, which may reflect underlying cellular and molecular processes that shape cortical maturation. Overall, our findings provide a better understanding of the heterogeneous and regionally specific maturational timeline of the functional connectome in typical development. This lays the groundwork for identifying brain-based biomarkers for atypical development indicated by altered neurodevelopmental trajectories in the brain's functional architecture.

Acknowledgments

The authors thank the families who generously gave their time to participate in this study.

Author contributions

Janelle Liu (Conceptualization, Data curation, Formal analysis, Investigation, Methodology, Visualization, Writing—original draft, Writing—review and editing), Haitao Chen (Data curation, Writing—review and editing), Emil Cornea (Data curation, Investigation, Project administration, Resources, Writing—review and editing), John H. Gilmore (Funding acquisition, Investigation, Project administration, Resources, Supervision, Writing—review and editing), Wei Gao (Funding acquisition, Investigation, Resources, Supervision, Writing—review and editing).

Funding

This work was supported by the National Institutes of Health (R34DA050255, R01DA042988, R01DA043678, R21NS088975, R21DA043171, and R03DA036645 to W.G.; R01MH064065 and R01HD05300 to J.H.G.) and by Cedars-Sinai Precision Medicine Initiative Award and institutional support (to W.G.).

Conflict of interest statement: None declared.

Data availability

Due to confidentiality reasons, data used in this manuscript can be requested and shared after University of North Carolina–Chapel Hill and Cedars-Sinai Medical Center IRB review and necessary data sharing agreement being established.

Supplementary material

Supplementary material is available at *Cerebral Cortex* online.

References

Alcauter S, Lin W, Keith Smith J, Gilmore JH, Gao W. Consistent anterior-posterior segregation of the insula during the first 2 years of life. *Cereb Cortex*. 2015:25(5):1176–1187.

Apps MAJ, Rushworth MFS, Chang SWC. The anterior cingulate gyrus and social cognition: tracking the motivation of others. *Neuron*. 2016:90(4):692–707.

Atzil S, Gao W, Fradkin I, Barrett LF. Growing a social brain. *Nat Hum Behav*. 2018:2(9):624–636. Available at https://www.nature.com/articles/s41562-018-0384-6 [Accessed 2022 November 1].

Avants BB, Epstein CL, Grossman M, Gee JC. Symmetric diffeomorphic image registration with cross-correlation: evaluating automated labeling of elderly and neurodegenerative brain. *Med Image Anal*. 2008:12(1):26–41.

Benjamini Y, Hochberg Y. Controlling the false discovery rate: a practical and powerful approach to multiple testing. *J R Stat Soc Ser B*. 1995:57(1):289–300. Available at https://onlinelibrary.wiley.com/doi/full/10.1111/j.2517-6161.1995.tb02031.x [Accessed 2022 November 1].

Bosch-Bayard J, Biscay RJ, Fernandez T, Otero GA, Ricardo-Garcell J, Aubert-Vazquez E, Evans AC, Harmony T. EEG effective connectivity during the first year of life mirrors brain synaptogenesis, myelination, and early right hemisphere predominance. *NeuroImage*. 2022:252:119035.

Bouret S, Richmond BJ. Ventromedial and orbital prefrontal neurons differentially encode internally and externally driven motivational values in monkeys. *J Neurosci*. 2010:30(25):8591–8601.

Braun U, Plichta MM, Esslinger C, Sauer C, Haddad L, Grimm O, Mier D, Mohnke S, Heinz A, Erk S, et al. Test-retest reliability of resting-state connectivity network characteristics using fMRI and graph theoretical measures. *NeuroImage*. 2012:59(2):1404–1412.

Burgos-Robles A, Gothard KM, Monfils MH, Morozov A, Vicentic A. Conserved features of anterior cingulate networks support observational learning across species. *Neurosci Biobehav Rev*. 2019:107:215–228.

Carmichael ST, Price JL. Sensory and premotor connections of the orbital and medial prefrontal cortex of macaque monkeys. *J Comp Neurol*. 1995:363(4):642–664. Available at https://onlinelibrary.wiley.com/doi/full/10.1002/cne.903630409 [Accessed 2022 October 25].

Chen H, Liu J, Chen Y, Salzwedel A, Cornea E, Gilmore JH, Gao W. Developmental heatmaps of brain functional connectivity from newborns to 6-year-olds. *Dev Cogn Neurosci*. 2021a:50:100976. https://doi.org/10.1016/j.dcn.2021.100976.

Chen Y, Liu S, Salzwedel A, Stephens R, Cornea E, Goldman BD, Gilmore JH, Gao W. The subgrouping structure of newborns with heterogeneous brain-behavior relationships. *Cereb Cortex*. 2021b:31(1):301–311.

Conway BR. The organization and operation of inferior temporal cortex. *Annu Rev Vis Sci*. 2018:4(1):381–402.

Cox RW. AFNI: software for analysis and visualization of functional magnetic resonance neuroimages. *Comput Biomed Res*. 1996:29(3):162–173. Available at https://ac-els-cdn-com.ezp-prod1.hul.harvard.edu/S0010480996900142/1-s2.0-S0010480996900142-main.pdf?_tid=c22bae7a-b8f5-4a8b-9dac-91c1ed841d53&acdnat=1549393398_e37181b8933a2ac88c2d7dc0eab14413.

Curran PJ, Obeidat K, Losardo D. Twelve frequently asked questions about growth curve modeling. *J Cogn Dev*. 2010:11(2):121–136.

Cusack R, McCuaig O, Linke AC. Methodological challenges in the comparison of infant fMRI across age groups. *Dev Cogn Neurosci*. 2018:33:194–205. https://doi.org/10.1016/j.dcn.2017.11.003.

De Asis-Cruz J, Andescavage N, Limperopoulos C. Adverse prenatal exposures and fetal brain development: insights from advanced fetal magnetic resonance imaging. *Biol Psychiatry Cogn Neurosci Neuroimaging*. 2022:7(5):480–490.

De Haas B, Sereno MI, Schwarzkopf DS. Behavioral/cognitive inferior occipital gyrus is organized along common gradients of spatial and face-part selectivity. *J Neurosci*. 2021:41(25):5511–5521. https://doi.org/10.1523/JNEUROSCI.2415-20.2021 [Accessed 2022 November 1].

DeMaster D, Bick J, Johnson U, Montroy JJ, Landry S, Duncan AF. Nurturing the preterm infant brain: leveraging neuroplasticity

to improve neurobehavioral outcomes. *Pediatr Res*. 2019:85(2): 166–175.

Dufford AJ, Spann M, Scheinost D. How prenatal exposures shape the infant brain: insights from infant neuroimaging studies. *Neurosci Biobehav Rev*. 2021:131:47–58. https://doi.org/10.1016/j.neubiorev.2021.09.017.

Ellis CT, Turk-Browne NB. Infant fMRI: a model system for cognitive neuroscience. *Trends Cogn Sci*. 2018:22(5):375–387.

Emerson RW, Gao W, Lin W. Longitudinal study of the emerging functional connectivity asymmetry of primary language regions during infancy. *J Neurosci*. 2016:36(42):10883–10892.

Fair DA, Cohen AL, Power JD, Dosenbach NUF, Church JA, Miezin FM, Schlaggar BL, Petersen SE. Functional brain networks develop from a "local to distributed" organization. *PLoS Comput Biol*. 2009:5(5):14–23.

Fransson P, Skiöld B, Horsch S, Nordell A, Blennow M, Lagercrantz H, Åden U. Resting-state networks in the infant brain. *Proc Natl Acad Sci U S A*. 2007:104(39):15531–15536. Available at www.pnas.org/cgi/content/full/ [Accessed 2022 November 1].

Fransson P, Skiöld B, Engström M, Hallberg B, Mosskin M, Åden U, Lagercrantz H, Blennow M. Spontaneous brain activity in the newborn brain during natural sleep-an fMRI study in infants born at full term. *Pediatr Res*. 2009:66(3):301–305.

Fransson P, Åden U, Blennow M, Lagercrantz H. The functional architecture of the infant brain as revealed by resting-state fMRI. *Cereb Cortex*. 2011:21(1):145–154.

Gao W, Zhu H, Giovanello KS, Smith JK, Shen D, Gilmore JH, Lin W. Evidence on the emergence of the brain's default network from 2-week-old to 2-year-old healthy pediatric subjects. *Proc Natl Acad Sci U S A*. 2009:106(16):6790–6795.

Gao W, Gilmore JH, Giovanello KS, Smith JK, Shen D, Zhu H, Lin W. Temporal and spatial evolution of brain network topology during the first two years of life. *PLoS One*. 2011:6(9):e25278.

Gao W, Alcauter S, Elton A, Hernandez-Castillo CR, Smith JK, Ramirez J, Lin W. Functional network development during the first year: relative sequence and socioeconomic correlations. *Cereb Cortex*. 2015a:25(9):2919–2928.

Gao W, Alcauter S, Smith JK, Gilmore JH, Lin W. Development of human brain cortical network architecture during infancy. *Brain Struct Funct*. 2015b:220(2):1173–1186.

Gao W, Lin W, Grewen K, Gilmore JH. Functional connectivity of the infant human brain: Plastic and modifiable. *Neuroscientist*. 2017:23(2):169–184.

Gao W, Grewen K, Knickmeyer RC, Qiu A, Salzwedel A, Lin W, Gilmore JH. A review on neuroimaging studies of genetic and environmental influences on early brain development. *NeuroImage*. 2019:185: 802–812. https://doi.org/10.1016/j.neuroimage.2018.04.032.

Gilmore JH, Knickmeyer RC, Gao W. Imaging structural and functional brain development in early childhood. *Nat Rev Neurosci*. 2018:19(3):123–137. https://doi.org/10.1038/nrn.2018.1.

Graham AM, Pfeifer JH, Fisher PA, Lin W, Gao W, Fair DA. The potential of infant fMRI research and the study of early life stress as a promising exemplar. *Dev Cogn Neurosci*. 2015:12: 12–39.

Graven SN, Browne JV. Sensory development in the fetus, neonate, and infant: introduction and overview. *Newborn Infant Nurs Rev*. 2008:8(4):169–172.

Grayson DS, Fair DA. Development of large-scale functional networks from birth to adulthood: A guide to the neuroimaging literature. *NeuroImage*. 2017:160:15–31. https://doi.org/10.1016/j.neuroimage.2017.01.079.

Hartwigsen G, Baumgaertner A, Price CJ, Koehnke M, Ulmer S, Siebner HR. Phonological decisions require both the left and right supramarginal gyri. *Proc Natl Acad Sci U S A*. 2010:107(38): 16494–16499.

Holroyd CB, Verguts T. The best laid plans: computational principles of anterior cingulate cortex. *Trends Cogn Sci*. 2021:25(4): 316–329.

Hong J-H, Park M. Understanding synaptogenesis and functional connectome in *C. elegans* by imaging technology. *Front Synaptic Neurosci*. 2016:8:18. https://doi.org/10.3389/fnsyn.2016.00018.

Huttenlocher PR. Synapse elimination and plasticity in developing human cerebral cortex. *Am J Ment Defic*. 1984:88(5): 488–496.

Huttenlocher PR. Morphometric study of human cerebral cortex development. *Neuropsychologia*. 1990:28(6):517–527.

Joshi AA, Chong M, Li J, Choi S, Leahy RM. Are you thinking what I'm thinking? Synchronization of resting fMRI time-series across subjects. *NeuroImage*. 2018:172:740–752.

Kelly AMC, Di Martino A, Uddin LQ, Shehzad Z, Gee DG, Reiss PT, Margulies DS, Castellanos FX, Milham MP. Development of anterior cingulate functional connectivity from late childhood to early adulthood. *Cereb Cortex*. 2009:19(3):640–657. Available at https://academic.oup.com/cercor/article/19/3/640/434704.

Keunen K, Counsell SJ, Benders MJNL. The emergence of functional architecture during early brain development. *NeuroImage*. 2017:160:2–14.

Kovacs-Balint ZA, Payne C, Steele J, Li L, Styner M, Bachevalier J, Sanchez MM. Structural development of cortical lobes during the first 6 months of life in infant macaques. *Dev Cogn Neurosci*. 2021:48:100906.

Lee W, Morgan BR, Shroff MM, Sled JG, Taylor MJ. The development of regional functional connectivity in preterm infants into early childhood. *Neuroradiology*. 2013:55(S2):105–111.

Liu X, Somel M, Tang L, Yan Z, Jiang X, Guo S, Yuan Y, He L, Oleksiak A, Zhang Y, et al. Extension of cortical synaptic development distinguishes humans from chimpanzees and macaques. *Genome Res*. 2012:22(4):611–622. Available at http://www.genome.org/cgi/doi/10.1101/gr.127324.111 [Accessed 2023 May 16].

Liu J, Chen Y, Stephens R, Cornea E, Goldman B, Gilmore JH, Gao W. Hippocampal functional connectivity development during the first two years indexes 4-year working memory performance. *Cortex*. 2021:138:165–177. https://doi.org/10.1016/j.cortex.2021.02.005.

McCormick EM. Multi-level multi-growth models: new opportunities for addressing developmental theory using advanced longitudinal designs with planned missingness. *Dev Cogn Neurosci*. 2021:51:101001. https://doi.org/10.1016/j.dcn.2021.101001.

McCormick EM, Peters S, Crone EA, Telzer EH. Longitudinal network re-organization across learning and development. *NeuroImage*. 2021:229:117784. https://doi.org/10.1016/j.neuroimage.2021.117784.

Menon V, Uddin LQ. Saliency, switching, attention and control: a network model of insula function. *Brain Struct Funct*. 2010: 214(5–6):655–667.

Ongur D, Price JL. The organization of networks within the orbital and medial prefrontal cortex of rats, monkeys and humans. *Cereb Cortex*. 2000:10(3):206–219.

Ouyang M, Dubois J, Yu Q, Mukherjee P, Huang H. Delineation of early brain development from fetuses to infants with diffusion MRI and beyond. *NeuroImage*. 2019:185:836–850.

Palermo S, Stanziano M, Morese R. Commentary: anterior cingulate cortex and response conflict: effects of frequency, inhibition and errors. *Front Behav Neurosci*. 2018:12:1–2.

Pendl SL, Salzwedel AP, Goldman BD, Barrett LF, Lin W, Gilmore JH, Gao W. Emergence of a hierarchical brain during infancy

reflected by stepwise functional connectivity. *Hum Brain Mapp*. 2017:38(5):2666–2682.

Petanjek Z, Judaš M, Kostović I, Uylings HBM. Lifespan alterations of basal dendritic trees of pyramidal neurons in the human prefrontal cortex: a layer-specific pattern. *Cereb Cortex*. 2008:18(4): 915–929.

Petanjek Z, Judaš M, Šimić G, Rašin MR, Uylings HBM, Rakic P, Kostović I. Extraordinary neoteny of synaptic spines in the human prefrontal cortex. *Proc Natl Acad Sci U S A*. 2011:108(32): 13281–13286. Available at www.pnas.org/cgi/doi/10.1073/pnas.1105108108 [Accessed 2023 May 16].

Petanjek Z, Sedmak D, Džaja D, Hladnik A, Rašin MR, Jovanov-Milosevic N. The protracted maturation of associative layer IIIC pyramidal neurons in the human prefrontal cortex during childhood: a major role in cognitive development and selective alteration in autism. *Front Psych*. 2019: 10:122.

Pfeifer JH, Allen NB, Byrne ML, Mills KL. Modeling developmental change: contemporary approaches to key methodological challenges in developmental neuroimaging. *Dev Cogn Neurosci*. 2018:33:1–4.

Pollatou A, Filippi CA, Aydin E, Vaughn K, Thompson D, Korom M, Dufford AJ, Howell B, Zöllei L, Di Martino A, et al. An ode to fetal, infant, and toddler neuroimaging: chronicling early clinical to research applications with MRI, and an introduction to an academic society connecting the field. *Dev Cogn Neurosci*. 2022:54:101083.

Power JD, Barnes KA, Snyder AZ, Schlaggar BL, Petersen SE. Spurious but systematic correlations in functional connectivity MRI networks arise from subject motion. *NeuroImage*. 2012:59(3): 2142–2154. https://doi.org/10.1016/j.neuroimage.2011.10.018.

Power JD, Mitra A, Laumann TO, Snyder AZ, Schlaggar BL, Petersen SE. Methods to detect, characterize, and remove motion artifact in resting state fMRI. *NeuroImage*. 2014:84:320–341. https://doi.org/10.1016/j.neuroimage.2013.08.048.

Rakic P, Bourgeois JP, Goldman-Rakic PS. Synaptic development of the cerebral cortex: Implications for learning, memory, and mental illness. *Prog Brain Res*. 1994:102:227–243.

Redcay E, Warnell KR. A social-interactive neuroscience approach to understanding the developing brain. *Advances in Child Development and Behavior*. 2018:54:1–44. https://doi.org/10.1016/bs.acdb.2017.10.001.

Rogers CE, Lean RE, Wheelock MD, Smyser CD. Aberrant structural and functional connectivity and neurodevelopmental impairment in preterm children. *J Neurodev Disord*. 2018:10(1):38. https://doi.org/10.1186/s11689-018-9253-x [Accessed 2022 November 1].

Rolls ET, Cheng W, Feng J. The orbitofrontal cortex: reward, emotion and depression. *Brain Commun*. 2020:2(2):1–25.

Rudolph MD, Graham AM, Feczko E, Miranda-Dominguez O, Rasmussen JM, Nardos R, Entringer S, Wadhwa PD, Buss C, Fair DA. Maternal IL-6 during pregnancy can be estimated from newborn brain connectivity and predicts future working memory in offspring. *Nat Neurosci*. 2018:21(5):765–772. https://doi.org/10.1038/s41593-018-0128-y [Accessed 2023 March 3].

Salzwedel AP, Stephens RL, Goldman BD, Lin W, Gilmore JH, Gao W. SUPPLEMENT Development of amygdala functional connectivity during infancy and its relationship with 4-year behavioral outcomes. *Biol Psychiatry Cogn Neurosci Neuroimaging*. 2019a:4(1): 62–71.

Salzwedel AP, Stephens RL, Goldman BD, Lin W, Gilmore JH, Gao W. Development of amygdala functional connectivity during infancy and its relationship with 4-year behavioral outcomes. *Biol Psychiatry Cogn Neurosci Neuroimaging*. 2019b:4(1):62–71. https://doi.org/10.1016/j.bpsc.2018.08.010.

Sanchez CE, Richards JE, Almli CR. Age-specific MRI templates for pediatric neuroimaging. *Dev Neuropsychol*. 2012:37(5): 379–399.

Sato T, Uchida G, Lescroart MD, Kitazono J, Okada M, Tanifuji M. Object representation in inferior temporal cortex is organized hierarchically in a mosaic-like structure. *J Neurosci*. 2013:33(42): 16642–16656.

Sato W, Kochiyama T, Uono S, Matsuda K, Usui K, Inoue Y, Toichi M. Rapid, high-frequency, and theta-coupled gamma oscillations in the inferior occipital gyrus during face processing. *Cortex*. 2014:60:52–68.

Scheinost D, Finn ES, Tokoglu F, Shen X, Papademetris X, Hampson M, Todd Constable R. Sex differences in normal age trajectories of functional brain networks. *Hum Brain Mapp*. 2015:36(4):1524–1535. Available at https://onlinelibrary.wiley.com/doi/10.1002/hbm.22720 [Accessed 2022 November 28].

Scheinost D, Sinha R, Cross SN, Kwon SH, Sze G, Constable RT, Ment LR. Does prenatal stress alter the developing connectome? *Pediatr Res*. 2017:81(1–2):214–226.

Schneider KN, Sciarillo XA, Nudelman JL, Cheer JF, Roesch MR. Anterior cingulate cortex signals attention in a social paradigm that manipulates reward and shock. *Curr Biol*. 2020:30(19): 3724–3735.e2.

Shapira-Lichter I, Strauss I, Oren N, Gazit T, Sammartino F, Giacobbe P, Kennedy S, Hutchison WD, Fried I, Hendler T, et al. Conflict monitoring mechanism at the single-neuron level in the human ventral anterior cingulate cortex. *NeuroImage*. 2018:175:45–55. https://doi.org/10.1016/j.neuroimage.2018.03.028 [Accessed 2022 November 1].

Shi F, Yap PT, Wu G, Jia H, Gilmore JH, Lin W, Shen D. Infant brain atlases from neonates to 1- and 2-year-olds. *PLoS One*. 2011:6(4):e18746.

Shi F, Salzwedel AP, Lin W, Gilmore JH, Gao W. Functional brain parcellations of the infant brain and the associated developmental trends. *Cereb Cortex*. 2018:28(4):1358–1368.

Silani G, Lamm C, Ruff CC, Singer T. Right supramarginal gyrus is crucial to overcome emotional egocentricity bias in social judgments. *J Neurosci*. 2013:33(39):15466–15476.

Simmonds DJ, Hallquist MN, Luna B. Protracted development of executive and mnemonic brain systems underlying working memory in adolescence: a longitudinal fMRI study. *NeuroImage*. 2017:157:695–704.

Smith SM, Jenkinson M, Woolrich MW, Beckmann CF, Behrens TEJ, Johansen-Berg H, Bannister PR, De Luca M, Drobnjak I, Flitney DE, et al. Advances in functional and structural MR image analysis and implementation as FSL. *NeuroImage*. 2004:23:208–219.

Smyser CD, Inder TE, Shimony JS, Hill JE, Degnan AJ, Snyder AZ, Neil JJ. Longitudinal analysis of neural network development in preterm infants. *Cereb Cortex*. 2010:20(12):2852–2862.

Smyser CD, Snyder AZ, Neil JJ. Functional connectivity MRI in infants: exploration of the functional organization of the developing brain. *NeuroImage*. 2011:56(3):1437–1452. https://doi.org/10.1016/j.neuroimage.2011.02.073.

Solé-Padullés C, Castro-Fornieles J, De La Serna E, Calvo R, Baeza I, Moya J, Lázaro L, Rosa M, Bargalló N, Sugranyes G. Intrinsic connectivity networks from childhood to late adolescence: effects of age and sex. *Dev Cogn Neurosci*. 2016:17:35–44.

Stoeckel C, Gough PM, Watkins KE, Devlin JT. Supramarginal gyrus involvement in visual word recognition. *Cortex*. 2009:45(9): 1091–1096.

Supekar K, Musen M, Menon V. Development of large-scale functional brain networks in children. *PLoS Biol*. 2009:7(7):e1000157.

Telzer EH, McCormick EM, Peters S, Cosme D, Pfeifer JH, van Duijvenvoorde ACK. Methodological considerations for developmental longitudinal fMRI research. *Dev Cogn Neurosci*. 2018:33:149–160. https://doi.org/10.1016/j.dcn.2018.02.004.

Toga AW, Thompson PM, Sowell ER. Mapping brain maturation. *Trends Neurosci*. 2006:29(3):148–159.

Travis K, Ford K, Jacobs B. Regional dendritic variation in neonatal human cortex: a quantitative Golgi study. *Dev Neurosci*. 2005:27(5):277–287. Available at https://pubmed.ncbi.nlm.nih.gov/16137985/ [Accessed 2023 May 16].

Uddin LQ. Salience processing and insular cortical function and dysfunction. *Nat Rev Neurosci*. 2015:16(1):55–61. https://doi.org/10.1038/nrn3857.

Uddin LQ, Supekar K, Menon V. Typical and atypical development of functional human brain networks: insights from resting-state fMRI. *Front Syst Neurosci*. 2010:4:1–12.

van den Heuvel MP, Kersbergen KJ, De Reus MA, Keunen K, Kahn RS, Groenendaal F, De Vries LS, Benders MJNL. The neonatal connectome during preterm brain development. *Cereb Cortex*. 2015:25(9):3000–3013.

Van Dijk KRA, Hedden T, Venkataraman A, Evans KC, Lazar SW, Buckner RL. Intrinsic functional connectivity as a tool for human connectomics: theory, properties, and optimization. *J Neurophysiol*. 2010:103(1):297–321. Available at www.jn.org [Accessed 2023 May 18].

Wheelock MD, Hect JL, Hernandez-Andrade E, Hassan SS, Romero R, Eggebrecht AT, Thomason ME. Sex differences in functional connectivity during fetal brain development. *Dev Cogn Neurosci*. 2019:36:100632.

Yeo BT, Krienen FM, Sepulcre J, Sabuncu MR, Lashkari D, Hollinshead M, Roffman JL, Smoller JW, Zöllei L, Polimeni JR, et al. The organization of the human cerebral cortex estimated by intrinsic functional connectivity. *J Neurophysiol*. 2011:106(3):1125–1165.